Quantification of the influence of aerodynamic model assumptions for dynamic analyses of bridges

Igor Kavrakov, Guido Morgenthal

Bauhaus-University Weimar, Germany

Ahsan Kareem

University of Notre Dame, USA

Contact: igor.kavrakov@uni-weimar.de

Abstract

Long-span bridges are sensitive to wind-induced forces. In this paper, we evaluate the influence of the assumptions in the semi-analytical aerodynamic models on the dynamic response of a bridge deck using comparison metrics. These metrics are constructed in such way to evaluate the differences in the signal properties of the time-dependent response. The signal properties include the time-varying frequency and magnitude content, phase and stationarity. The behavior of the metrics is first studied on illustrative examples. Finally, the metrics are used to quantify the discrepancies in the response of a streamlined deck, obtained by utilizing a numerical and two semi-analytical models. The results of the study provide deeper insight into bridge aerodynamics.

Keywords: long-span bridges; bridge aerodynamics; aeroelasticity; CFD; comparison metrics.

1 Introduction

With increasing spans of cable-supported bridges, the wind-induced vibrations become the most prominent action on such structures. A multitude of semi-analytical aerodynamic models are available to describe wind loads acting on a bridge deck [1]. In the past few decades, numerical models based on Computational Fluid Dynamics (CFD) have also emerged as an instrument for analysing the wind-structure interaction. Each semi-analytical model for the aerodynamic forces is based on a set of assumptions such as aerodynamic linearity and quasi-steadiness; therefore, these models cannot account for all the phenomena simultaneously for the whole range of reduced velocities. The need to quantify the influence of the assumptions implied within the aerodynamic models on the deck response becomes apparent for slender bridges, in order to make an accurate prediction of the wind loading. Commonly, the comparison of the semi-analytical aerodynamic models in the time-domain is performed by subjecting the structural system to an identical wind fluctuating velocities and monitoring the displacements. There has been several studies (cf. e.g. [1,2]), which compare the semi-analytical models by taking the root-mean-square (RMS) of the displacements as a quantity of interest. However, the RMS is an averaged quantity, which is not the best indicator of the nonlinear and non-stationary features of a signal.

Therefore, in this study, we apply comparison metrics for assessment of particular features of two response time histories. These features include the relative differences in phase, peak, RMS, time- and frequency-dependent magnitude, stationarity and nonlinear features. Based on the

results of the comparison metrics, a multicriteria assessment of the effect of assumptions implied in the aerodynamic models is performed. A comparison of two time histories has been commonly performed utilizing the validation metrics in vehicle safety applications [3]. Some of the metrics used herein are adapted from the validation metrics. In fact, the validation metrics are comparison metrics, in which the reference model is experimental one.

The article is organized as follows: In Sec. 2 we introduce the mathematical construction of the comparison metrics. The metrics are applied on basic examples to study their performance in Sec. 3. Section 4 presents the results of the metrics for the response of a bridge deck. Finally, we make concluding remarks in Sec. 5.

2 Comparison Metrics

Considering two signals $x = x(t)$ and $y = y(t)$ dependent on time t and with equal length T, we denote a comparison metric as $M = M(x, y)$, where x is a reference signal. The metrics are constructed in such way that their values are between 0 and 1, the latter identifying that there are no discrepancies in the signal property of interest. To facilitate this, we construct the metrics using an exponential function with negative exponent as:

$$M(x, y) = \exp(-\lambda |A(x, y)|), \tag{1}$$

where λ is the metric parameter and $A(x, y)$ is a relative exponent which is constructed in such manner to account a particular property of the signals. The metric parameter is introduced to adjust the sensitivity of the metrics. For simplicity, herein the metric parameter amounts to λ=1. A total of eight metrics are considered, including: (i) phase M_φ, (ii) peak M_p, (iii) RMS M_{rms}, (iv) magnitude M_m, (v) wavelet M_w, (vi) frequency normalized wavelet M_{wf}, (vii) stationarity M_S and (viii) bicoherence M_{b} metrics.

The phase metric accounts for mean phase discrepancy, and its relative exponents yields [3]:

$$A_\varphi = \frac{t_{lag}}{T_c}, \tag{2}$$

where t_{lag} is the time delay. The time delay is obtained as argument of the maxima of the cross-correlation between the two signals as:

$$t_{lag} = \arg\max_{\mathrm{t}} x(t) \star y(t). \tag{3}$$

The coefficient T_c is case-dependent and it is selected based on what is considered to be large delay between the studied signals.

The relative exponent for the peak metric is simply the relative difference between the two peaks of the signals, which yields:

$$A_p = \frac{\max_t |x(t)| - \max_t |y(t)|}{\max_t |x(t)|}. \tag{4}$$

In bridge aerodynamics, the RMS of a signal is an important quantity, as the incoming wind fluctuations are generally assumed to be stationary and Gaussian, while a linear aerodynamic model is utilized commonly. The relative exponent for the RMS metric is given as:

$$A_{\mathrm{rms}} = \frac{\sqrt{\int_0^T [x(t)]^2 \mathrm{d}t} - \sqrt{\int_0^T [y(t)]^2 \mathrm{d}t}}{\sqrt{\int_0^T [x(t)]^2 \mathrm{d}t}}. \tag{5}$$

The preceding metrics are based on an averaged quantity of the two signals. To further study the discrepancies in the time-localized magnitude of the signals, the relative exponent magnitude metric is formulated as [3]:

$$A_{\mathrm{m}} = \sqrt{\frac{\sum_{i=1}^{N_w} (x_w[i] - y_w[i])^2}{\sum_{i=1}^{N_w} (x_w[i])^2}}, \tag{6}$$

where $x_w = x_w[n]$, and $y_w = y_w[n]$ for $n \in \{1, 2, \dots, N_w\}$ are the discrete and warped signals of $x(t)$ and y(t), respectively, and N_w is the number of warped steps. The warped signals are obtained using the Dynamic Time Warping (DTW) algorithm. The DTW algorithm aligns the peaks of the signals by stretching, but not scaling [3]. Since we are interested only in the relative magnitude for M_m, we use the warped signals in order to minimize for the local discrepancies in the frequency and phase. The effect of DTW will be shown on an illustrative example in Sec. 3.

To account for the local discrepancies in the time-frequency plane, the wavelet metric is introduced.

The relative exponent for this metric is obtained by normalizing the integrated difference of the magnitude of the wavelet coefficients $W_x(a,t)$ and $W_x(a,t)$ in the time-frequency plane as:

$$A_w = \frac{\int_0^\infty \int_0^T ||W_x(a,t)|-|W_y(a,t)|| \mathrm{d}t\mathrm{d}a}{\int_0^\infty \int_0^T |W_x(a,t)| \mathrm{d}t\mathrm{d}a}, \quad (7)$$

where the $W_x(a,t)$ for $x(t)$ are obtained as:

$$W_x(a,t) = \frac{1}{\sqrt{|a|}} \int_{-\infty}^{\infty} x(\tau)\psi\left(\frac{t-\tau}{a}\right) \mathrm{d}\tau \quad (8)$$

where a is the scale and ψ is the parent wavelet. As a parent wavelet, herein we utilize the Morlet wavelet, for which the a is inversely proportional of the frequency f as $f \cong f_0/a$ and f_0 is the wavelet's central frequency.

The wavelet metric incorporates the total discrepancy in the time-frequency plane. To further illuminate whether this discrepancy is due to the amplitude or frequency difference, we introduce the frequency normalized wavelet metric, for which the relative exponent yields as:

$$A_{wf} = \int_0^T \frac{\int_0^\infty \left| \frac{|W_x(a,t)|}{\max_a |W_x(a,t)|} - \frac{|W_y(a,t)|}{\max_a |W_y(a,t)|} \right| \mathrm{d}a}{\int_0^\infty \frac{|W_x(a,t)|}{\max_a |W_x(a,t)|} da} \mathrm{d}t. \quad (9)$$

Practically, in M_{wf} we look at the discrepancies in the normalized instantaneous spectra. If value of M_{wf}=1 and M_w<1, the discrepancies in the signals are mainly in the amplitude while the relative frequency content of the signals is similar. This will be further discussed in the following section.

Another property, which is of interest in bridge aeroelasticity, is the stationarity of the response [4]. The stationarity metric is introduced herein, in order to identify whether both of the signals share the same property of stationarity. If both are non-stationary, M_s quantifies the discrepancies in the nonstationary part of the signals. To facilitate this, we formulate the relative exponent as a function of a stationarity index d as:

$$A_S \begin{cases} \to \infty & \text{if} \quad d_x \neq d_y, \\ = 0 & \text{if} \quad d_x = d_y = 0, \\ = \frac{\int_0^\infty \int_0^T \left| |W_x^F(a,t)| - |W_y^F(a,t)| \right| \mathrm{d}t\mathrm{d}a}{\int_0^\infty \int_0^T |W_x^F(a,t)| \mathrm{d}t\mathrm{d}a} & \text{if} \quad d_x = d_y = 1. \end{cases} \quad (10)$$

The stationarity index $d_x = d(x)$ take value of 0 if $x(t)$ is stationary and value of 1 otherwise. The determination of this index is based on discriminating test statistics between the signal $x(t)$ and stationary surrogate signals. In this case, the discriminating statistics are based on Log-spectral deviation. If the stationarity tests indicate that both signals are non-stationarity, the third condition in Eq. 10 is used to evaluate the discrepancies only in the non-stationary part of t wavelet magnitude $|W_x^F(a,t)|$. This part is obtained by filtering the wavelet coefficients, utilizing a threshold value for the spectrogram as:

$$W_x^F(a,t) = \begin{cases} 0 & if \quad S_x(a,t) < S_{\mathrm{tr}}(a,t), \\ W_x(a,t) & if \quad S_x(a,t) \geq S_{\mathrm{tr}}(a,t), \end{cases} \quad (11)$$

where $S_x = |W_x(a,t)|^2$ is the spectrogram of $x(t)$ and S_{tr} is the threshold value based on the surrogate signals. For further information on the filtering and stationarity test, we refer to [4].

Finally, the last metric utilized herein is based on the bicoherence $b_x(f_1,f_2)$. The bicoherence has been utilized in bridge aerodynamics recently, to identify some nonlinear features such as higher order harmonics in the forces [5] and is defined as

$$b_x(f_1,f_2) = \frac{|E[X(f_1)X(f_2)X^*(f_1+f_2)]|^2}{E[|X(f_1)X(f_2)|^2]E[|X^*(f_1+f_2)|^2]} \quad (12)$$

where $E[\cdot]$ denotes the expectation operator and $X(f)$ is the Fourier transform of $x(t)$. The relative exponent of A_{b} then yields:

$$A_b \begin{cases} \to \infty & if \quad k_x \neq k_y \\ = 0 & if \quad k_x = k_y \end{cases} \quad (13)$$

where the index k_x=1 if $b_x(f_1,f_2) \geq \varepsilon$, and 0 otherwise. The threshold $\varepsilon \in [0,1]$ is defined to filter the noise. Although an additional condition to quantify the nonlinear coupling can be introduced as in the third condition in Eq. (10), it was realized that the bicoherence is highly sensitive to noise and linear periodic components at $f_3 = f_1 + f_2$. Therefore, for now we use M_{b} only to identify if there are nonlinear features in one or both signals. To quantify the discrepancies in the nonlinear features, it is intended in the future to use the wavelet bicoherence to alleviate some of the difficulties in the bicoherence due to noise and the Heisenberg principle.

3 Illustrative examples

In this section, we study the comparison metrics for four basic signals with respect to a reference one and track their behaviour by changing certain signal properties. The considered reference (x_r) and basic signals (x_i) are given as:

$$
\begin{aligned}
x_r &= \mathrm{A}_1\cos(\omega_1 t) + A_2\cos\left(\omega_2 t + \tfrac{\pi}{3}\right) + \eta_1(t),\\
x_1 &= \mathrm{A}_1\cos(\omega_1 t + \varphi_1) + A_2\cos\left(\omega_2 t + \tfrac{\pi}{3} + \varphi_2\right) + \eta_2(t),\\
x_2 &= 2\mathrm{A}_1\cos(\omega_1 t) + 2A_2\cos\left(\omega_2 t + \tfrac{\pi}{3}\right) + \eta_3(t),\\
x_3 &= \mathrm{A}_1\cos(\omega_1 t) + A_2\cos\left(\omega_2 t + Kt^2 + \tfrac{\pi}{3}\right) + \eta_3(t),\\
x_4 &= \mathrm{A}_1\cos(\omega_1 t) + A_2\cos\left(\omega_2 t + \frac{\pi}{3}\right),\\
&\quad + \frac{(A_1 + A_2)}{2}\cos(\omega_1 t)\cos\left(\omega_2 t + \frac{\pi}{3}\right) + \eta_4(t),
\end{aligned}
\tag{14}
$$

where A_1=1; A_2=1.3; ω_1=2×2π; ω_2=2.8×2π; φ_1= π; φ_2= π/6; $K = (\omega_3 - \omega_2)/2T$; ω_3=3.6×2π and T is the signal length and η is white noise with small amplitude and zero mean. The reference value for the phase metric is chosen as T_c=π /ω_2.

By studying x_1 and x_r, we realize the effect of phase-shift, different for both harmonics, on the comparison metrics (cf. Figure 1). This example is chosen as a phase lag is a common manifestation of the fluid memory for the unsteady aerodynamic models. As expected, M_φ results in a lower value. In Figure 2, a sample time histories of original and warped signals are shown. It is noteworthy to mention that in this case, the magnitude metric obtained using the warped signals results in value of 0.88. Using the unwarped signals, M_m amounts to a value of 0.27, which is unrealistic as the signals are only shifted. Due to the added noise, the wavelet metrics, M_w and M_{wf}, result in values slightly less than 1. Considering the rest of the metrics, the signals are similar.

The second example is constructed in such way to study the amplitude difference. The amplitude of the signal x_2 is two times larger than x_r. Increasing the amplitude 100 % in such way, affects the RMS, magnitude, peak, wavelet metrics (cf. Figure 2). With exception of the magnitude metric, the rest of the metrics amounts to approx. 0.4, which is logical as exp(-1)≈0.37. A notable observation is that the value of the frequency normalized wavelet metric M_{wf}, remains 1. To further study this effect, the normalized wavelet magnitude of both signals is depicted in Figure 4. It is clear that the relative frequency content is similar for both signals. As expected, the phase, stationarity and bicoherence metrics amount to 1. The quasi-steady aerodynamic nonlinearity of the buffeting forces is commonly manifested through amplitude dependence.

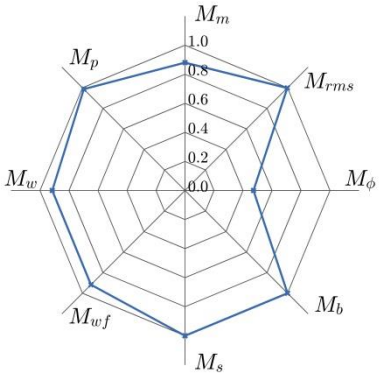

Figure 1. Comparison metrics $M(x_r, x_1)$

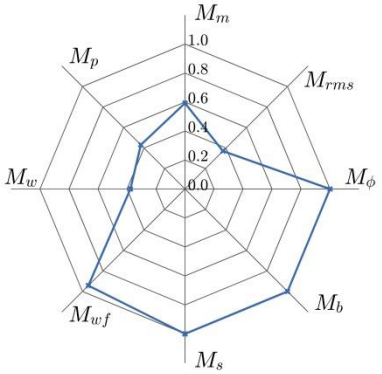

Figure 3. Comparison metrics $M(x_r, x_2)$

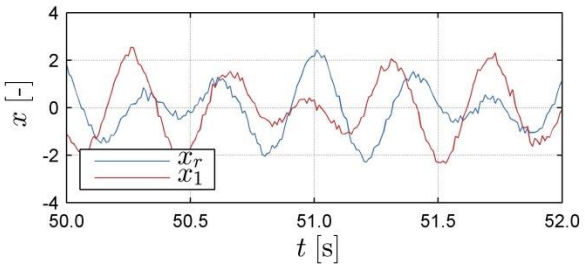

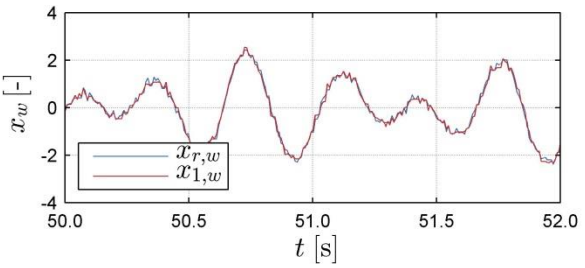

Figure 2. Sample time history of x_r and x_1 (left) and corresponding warped time histories of $x_{r,w}$ and $x_{1,w}$ (right)

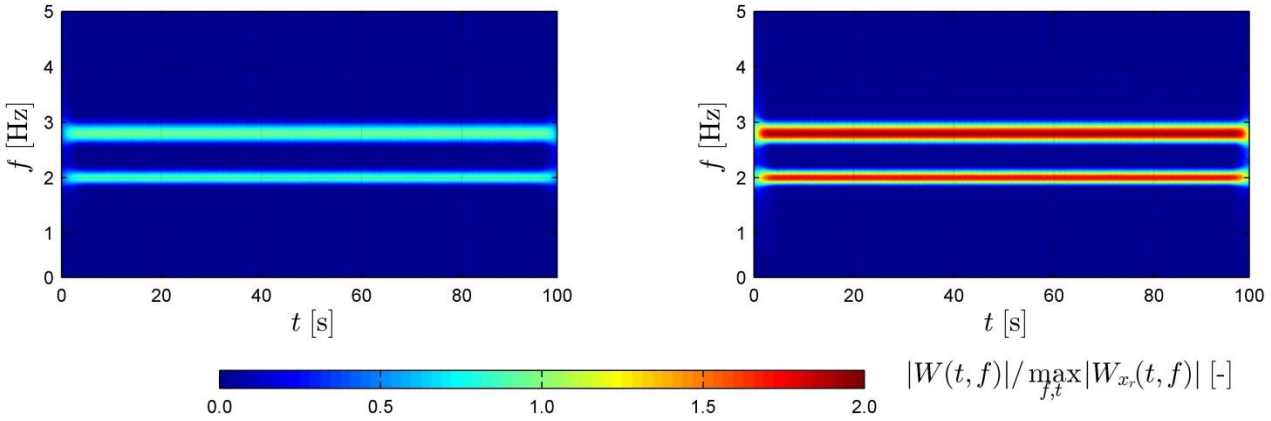

Figure 4. Wavelet magnitude of x_r (left) and x_2 (right), normalized with the maximum magnitude of x_r

In the third example, we study the effect of frequency modulation of one of the harmonics of the reference signal. The signal x_3 is practically a linear chirp, where the frequency is modulated. As expected, the stationarity metric is 0 (cf. Figure 5), as x_3 is a nonstationary signal, which could be seen as well in the wavelet magnitude in Figure 6. It is noteworthy to mention that while the wavelet based metrics result in low values, the peak and RMS metrics are close to 1. This further reinforces the claim why multicritera assessment is required

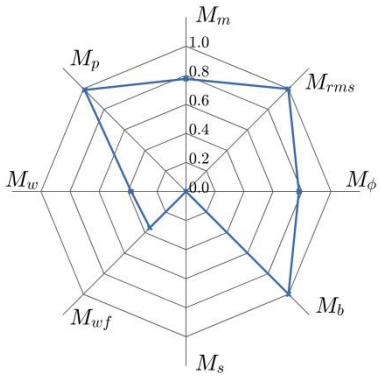

Figure 5. *Comparison metrics $M(x_r, x_3)$*

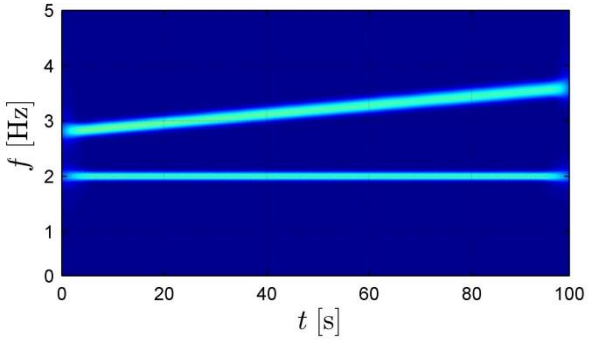

Figure 6. Normalized wavelet magnitude of x_3.The colour bar is identical as in Figure 4

beyond discussions based on the magnitude. Unlike the previous example, M_{wf} has similar value as M_w, which brings the conclusion that the discrepancies in M_w are due to relative frequency modulations, rather than amplitudes.

The last example is constructed as such to include a quadratic phase coupling between the two harmonics. Figure 7 depicts the comparison metrics for x_r and x_4. It is obvious that the nonlinear interaction influences mostly the magnitude metrics, and the bicoherence metric is zero. The spectrogram of x_4 (not shown) indicated additional two frequencies at f_1+ f_2 and f_2- f_1. However, from the bicoherence it is easy realize that these frequencies are a product of nonlinear interaction (cf. Figure 8). Looking at the bicoherence magnitude, it is clear that the corresponding frequency couples for x_4 are due to nonlinear interaction, as the bicoherence for the reference signal is trivial due to noise. As noted in [5], the bicoherence is useful for identifying higher order harmonics in bridge aerodynamics. Nevertheless, because of the large amount of divisions of each time history for the expectation

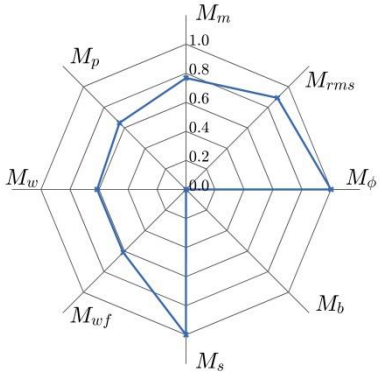

Figure 7. Comparison metrics $M(x_r, x_4)$

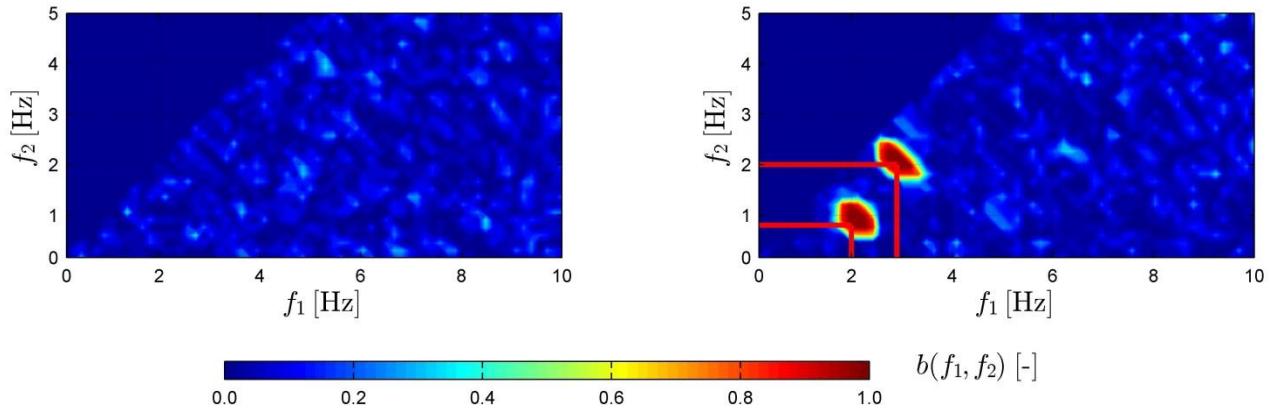

Figure 8. Bicoherence of x_r (left) and x_4 (right). The red lines indicate frequency couples: (f_1,- f_2) and (f_2, f_1)

operator in Eq. (12), the identification of nonlinear features would be probably more reliable if it is based on the wavelet bicoherence.

4 Application to bridge aeroelasticity

After studying the behaviour of the comparison metrics on basic examples, in this section we apply these metrics on a practical example from bridge aeroelasticity. The quantity of interest is the aeroelastic response of a two-dimensional bridge deck, which is immersed in a turbulent flow. For simplicity, the structural system is considered to have a vertical h and torsional α degree of freedom. The reference deck section is similar to the one of the Great Belt bridge, which is a 31 m wide streamlined box girder (cf. Figure 9). The mass and mass moment of inertia are set as 22.74 t/m and 2.47×10^3 tm^2/m, respectively, while the first vertical and torsional frequencies are 0.100 Hz and 0.278 Hz, respectively. A structural damping ratio of 0.5% of the critical damping is selected for all analyses.

The aeroelastic analyses are performed under a turbulent wind, utilizing a CFD model and two semi-analytical models. Wind speeds in the range of U=20-60 m/s are considered, with 6% isotropic turbulence intensity. The vortex particle method is utilized for the discretization of the Navier-Stokes equations for the CFD model, including free-stream turbulence [6]. As semi-analytical models for the aerodynamic forces, the Linear Unsteady (LU) and Quasi-steady (QS) models are considered. The LU model is linear and accounts for the fluid memory, while the QS model is nonlinear and disregards the fluid memory. Further information and mathematical formulation on these models is given in [1]. Before subjecting the structure to the turbulent flow, a CFD simulation without a section is conducted in order to track the wind fluctuations at the section location.

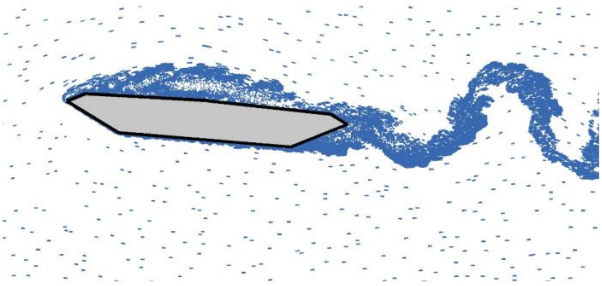

Figure 9. Sample particle map of bridge deck immersed in turbulent flow

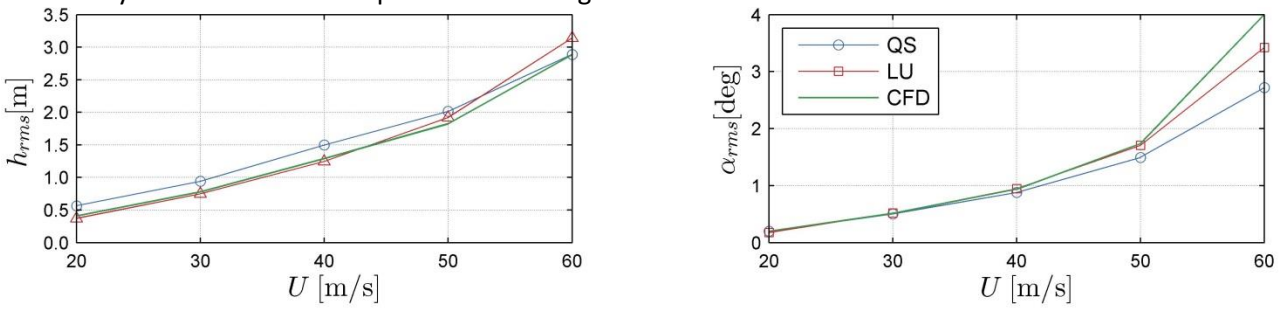

Figure 10. RMS of h (left) and α (right) under turbulent wind with 6% turbulence intensity

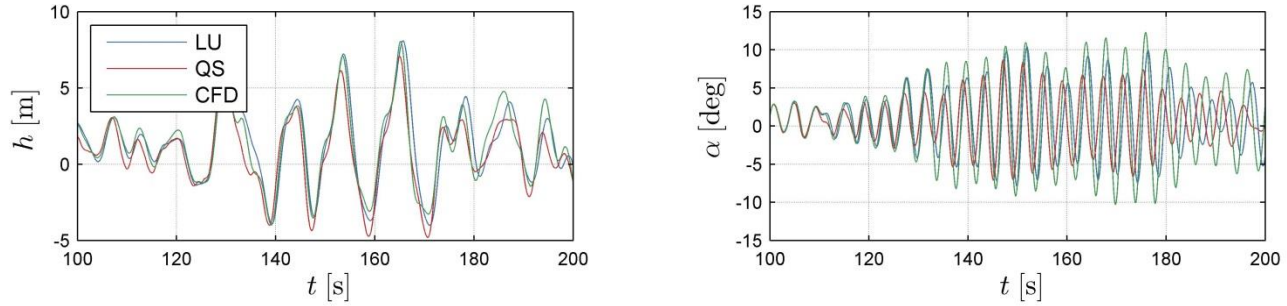

Figure 11. Sample time histories of the h (left) and α (right) at U= 60m/s with 6% turbulence intensity

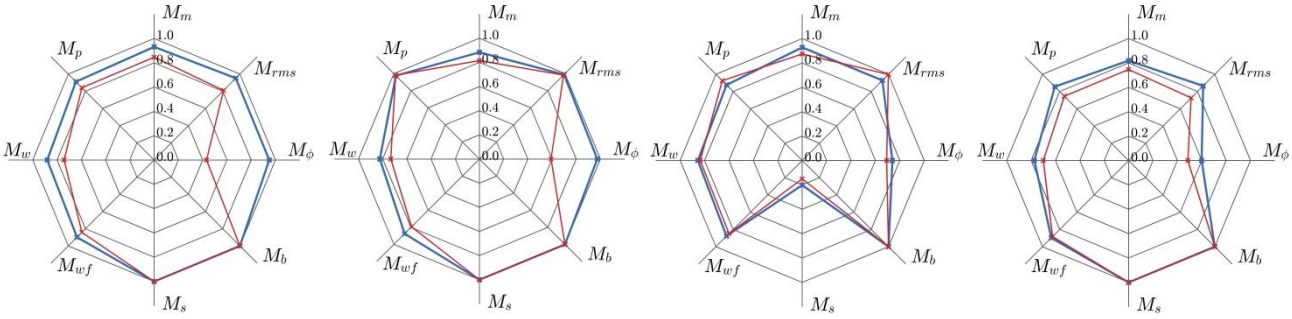

Figure 12. Comparison metrics $M(CFD, LU)$ (blue) and $M(CFD, QS)$ (red): U=30 m/s for h (left) and α (left-center); U=60 m/s for h (center-right) and α (right)

The tracked fluctuations serve as an input for the semi-analytical models, ensuring one-to-one comparison. The CFD model is taken as a reference in the following discussion.

For illustration, Figure 10 presents the RMS of the displacements for the selected models. Based on this figure, we can observe that in case of the vertical degree of freedom, the LU model performs better than the QS model, except at U=60 m/s. In case of the torsional displacements, the LU is closer to the reference than the QS model, especially at high wind speeds. Figure presents a sample time histories of the displacements at U= *60* m/s.

To further study the effect of fluid memory and quasi-steady nonlinearity, the comparison metrics are computed for two representative wind speeds of 30 m/s and 60 m/s (cf. Figure 12). Generally, the quasi-steady assumption is more rigorous than the linearity, as the comparison metrics for the LU models attain higher values than for the QS model. The quasi-steady assumption influences the phase significantly, although a difference is apparent for the high wind speed for the LU model. Looking the comparison metrics for h at U=60 m/s, we can realize why considering only the RMS as a metric is insufficient. Particularly, the QS model performs better for the RMS and the peak metrics. However, its performance is worse for the magnitude and wavelet-based metrics. This indicates that only the average quantities of the CFD model are in better correspondence with the QS model and not the local quantities. Since the input may be considered as identical, to draw a general conclusion that the quasi-steady nonlinearity is governing at high wind speeds, all metrics should support such statement. In this case, we may only indicate that the influence of the nonlinearity becomes apparent in the RMS and peak at high wind speeds. In Figure 13, the normalized wavelet magnitude for the α at U= *60* m/s is presented. It is noteworthy to notice, that M_{wf} is the same for both models, while M_w is worse for the QS model (cf. Figure 12). This indicates that the difference is due to magnitude underestimation, while that the relative frequency content is the same for the QS and LU models Another notable property for h at 60 m/s is that it features possible local nonstationarity. The stationarity index (cf. Eq. 10) resulted in 1 only for the LU model, for 95% confidence interval of Log-spectral deviation. Nevertheless, the filtered nonstationary part $|W^F|$ is computed using 99% confidence interval for all models (cf. Figure 14).

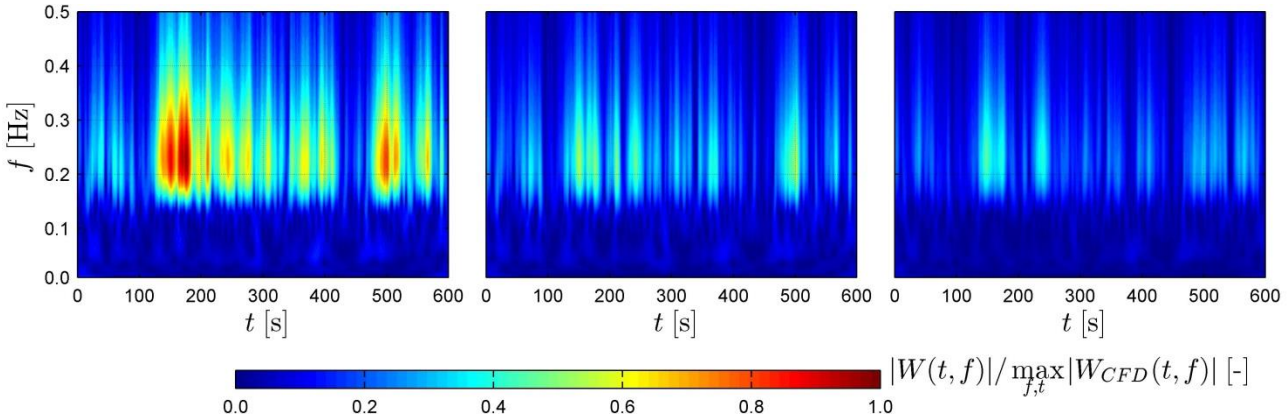

Figure 13. *Normalized wavelet magnitude of α at U=60 m/s for CFD (left), LU (center) and QS (right) models*

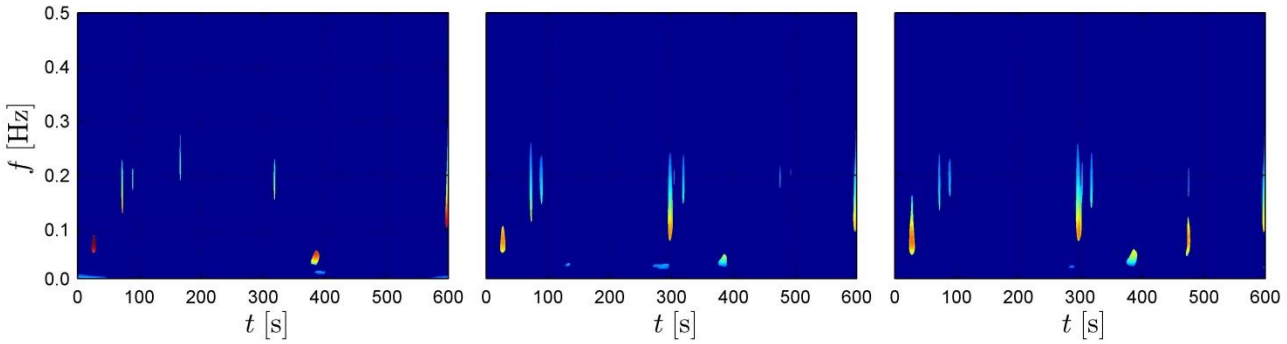

Figure 14. Filtered nonstationary part of the normalized wavelet magnitude $|W^F|$ of h at U=60 m/s for the CFD (left), LU (centre) and QS (right) models. The colour bar is identical as in Figure 13

Nonstationary "spikes" are visible for all models, indicating amplitude modulation. This could be attributed to initiation of divergent oscillations as the critical flutter velocity is ≈72 m/s for this case-study. The stationarity index is highly dependent on the discriminating statistic used and the filtering on the confidence interval; hence, further investigation on this regard is necessary

5 Summary and Conclusion

In summary, in this paper we studied the local and global discrepancies between time histories based on comparison metrics. Eight metrics were introduced based on the phase, magnitude, RMS, time dependent frequency content, stationarity and bicoherence. The metrics were initially examined on illustrative examples. This was followed by an examination of the response of a bridge deck due to wind excitation, to study the influence of the quasi-steady and linear assumptions.

In conclusion, the results indicate that multicriteria assessment of the time dependent response is necessary to study in-depth the influence of the assumptions, which are implied in the aerodynamic models. The metrics represent different signal properties and some of them are redundant. Therefore, an assessment should consider all metrics individually.

6 References

[1] Wu T., Kareem A. Bridge aerodynamics and aeroelasticity: a comparison of modeling schemes. *J Fluid Struct*. 2013; **43:** 347-370.

[2] Kavrakov I., Morgenthal G. A comparative assessment of aerodynamic models for buffeting and flutter of long-span bridges. *Eng*. 2017; **3:** 823-838.

[3] Sarin H., Kokkolaras M., Hulbert G., Papalambros P., Barbat S., Yang R.-J. Comparing time-histories for validation of simmulation models: Error measures and Metrics. *J Dyn Sys Meas Control*. 2010; **132**: 061401-061401-10.

[4] McCullough M., Kareem A. Testing stationarity with wavelet-based surrogates. *J Eng Mech.*2013; **139**: 200-209.

[5] Wu T., Kareem A. Aerodynamics and aeroelasticity of cable-supported bridges: Identification of nonlinear features. *J Eng Mech.* 2013; **139**: 1886-1893.

[6] Rassmusen J.T., Hejlesen M.M., Larsen A., Walther J.H. Discrete vortex method simulations of the aerodynamic admittance in bridge aerodynamics. *J Wind Eng Ind Aerodyn*. 2010; **98**: 754-766